

# Strangeness Production in Light and Intermediate size Nucleus-Nucleus Collisions

M.I. Gorenstein,<sup>1,2</sup> W. Greiner,<sup>2</sup> and A. Rustamov<sup>3</sup>

<sup>1</sup>*Bogolyubov Institute for Theoretical Physics, Kiev, Ukraine*

<sup>2</sup>*Frankfurt Institute for Advanced Studies, Frankfurt, Germany*

<sup>3</sup>*Goethe-University Frankfurt, Frankfurt, Germany*

## Abstract

Within the statistical model, the net strangeness conservation and incomplete total strangeness equilibration lead to the suppression of strange particle multiplicities. Furthermore, suppression effects appear to be stronger in small systems. By treating the production of strangeness within the canonical ensemble formulation we developed a simple model which allows to predict the excitation function of  $K^+/\pi^+$  ratio in nucleus-nucleus collisions. In doing so we assumed that different values of  $K^+/\pi^+$ , measured in p+p and Pb+Pb interactions at the same collision energy per nucleon, are driven by the finite size effects only. These predictions may serve as a baseline for experimental results from NA61/SHINE at the CERN SPS and the future CBM experiment at FAIR.

PACS numbers: 12.40.-y, 12.40.Ee

Keywords: nucleus-nucleus collisions, strangeness production

## I. INTRODUCTION

The multiplicity of pions per participating nucleon is known to be similar in nucleus-nucleus (A+A) and in inelastic proton-proton (p+p) interactions at the same collision energy per nucleon. This is in line with the Wounded Nucleon Model [1] (WNM) in which the final states in A+A collisions are treated as a superposition of independent nucleon-nucleon collisions. Similar picture emerges from the hadron statistical models within the grand canonical ensemble (GCE) formulation. At fixed temperature and chemical potentials all hadron multiplicities are proportional to the system volume  $V$ . Taking  $V$  to be proportional to the number of wounded nucleons  $N_W$  in A+A collisions, one restores the WNM results for hadron multiplicities.

Production of strange hadrons appears to be quite different in p+p and heavy-ion collisions. In particular, the ratio of  $K^+$  to  $\pi^+$  multiplicities is significantly larger in collisions of heavy ions. It was advocated to interpret this *strangeness enhancement* as a possible signature for the quark-gluon plasma creation [2]. A non-monotonic dependence of the  $K^+$  to  $\pi^+$  ratio as function of the collision energy (the *horn*) was predicted [3] as a fingerprint of the deconfinement phase transition. The predicted behavior was indeed observed by the NA49 Collaboration in central Pb+Pb collisions [4] at the SPS energies (for more details cf. Ref. [5]). Moreover, these findings have been recently confirmed by the RHIC and LHC data [6]. The experimental data on  $K^+/\pi^+$  ratio in p+p and Pb+Pb (Au+Au in the AGS energy range) collisions are presented in Fig. 1 as function of the center-of-mass energy of the nucleon pair  $\sqrt{s_{NN}}$  (for details see [7] and references therein).

Numbers of strange quarks  $N_s$  and antiquarks  $N_{\bar{s}}$  in a final state of p+p or A+A collisions are equal to each other due to the net strangeness conservation in strong interactions. In the SPS energy range strange quarks are essentially carried by  $K^-$ ,  $\bar{K}^0$  mesons and  $\Lambda$  hyperons. On the other hand, almost all  $N_{\bar{s}}$  created in the collision process are finally revealed in  $K^+$  and  $K^0$  particles. For the event averages one obtains an approximate relation  $\langle K^+ \rangle \cong 0.5 \langle N_{\bar{s}} \rangle$ . This explains the choice of the  $K^+$  multiplicity as an estimator for the total strangeness [5].

Conservation of strangeness in large statistical systems can be treated within the GCE formulation, in which all hadron multiplicities are proportional to the system volume  $V$ . In small systems, however, one has to follow the canonical ensemble (CE) treatment [8]. The

multiplicities of (anti)strange hadrons in CE decrease with decreasing volume faster than the GCE multiplicities.

A comparison of the statistical model results with hadron multiplicity data, within both CE and GCE, evidences an incomplete strangeness equilibration. For reasonable fit of the data one has to introduce the strangeness suppression factor  $\gamma_S$  [9]. Note that in p+p interactions the  $\gamma_S$  factor is smaller than in central Pb+Pb collisions [10].

In the present study the difference of the  $K^+/\pi^+$  ratio in p+p and Pb+Pb collisions is considered within the CE statistical model as a consequence of two strangeness suppression effects: (a) net strangeness conservation and (b) incomplete total strangeness equilibration. Our model assumes that both suppression effects depend on the system size and collision energy. Other physical differences between statistical systems created in p+p and Pb+Pb collisions which are not reduced to 'a' and 'b' are not considered. The finite-size strangeness suppression is then calculated in terms of two model parameters which are extracted from existing data on p+p and Pb+Pb collisions. This opens a possibility to make the model predictions for the  $K^+/\pi^+$  ratio in A+A collisions with light and intermediate ions. Such estimates are timely in view of experimental program of the NA61/SHINE at the CERN SPS [11]. The NA61/SHINE Collaboration has already recorded Be+Be data with projectile momenta of  $13A$ ,  $20A$ ,  $30A$ ,  $40A$ ,  $80A$ ,  $158A$  GeV/c. The energy scans with p+Pb, Ar+Ca and Xe+La collisions will be completed up to 2016. In addition, a beam energy scan of Pb+Pb collisions, with much higher statistics than that performed by the NA49 Collaboration, is planned. We hope that the atomic number dependence of the  $K^+/\pi^+$  ratio from p+p to Pb+Pb collisions in the SPS energy range may reveal new and important physical information.

The Letter is organized as follows. In Section II the strangeness suppression effects in the statistical systems are considered in the CE formulation. In Section III the model parameters are extracted from the data on p+p and Pb+Pb collisions. The model predictions of the  $K^+/\pi^+$  ratio for light and intermediate nucleus-nucleus collisions are calculated. Finally, Section IV summarizes the paper. Appendix A includes details of the calculations.

## II. STRANGENESS SUPPRESSION

We first introduce the following notations:

$$R_p \equiv \frac{\langle K^+ \rangle_{pp}}{\langle \pi^+ \rangle_{pp}}, \quad R_A \equiv \frac{\langle K^+ \rangle_{AA}}{\langle \pi^+ \rangle_{AA}}, \quad R_{Pb} \equiv \frac{\langle K^+ \rangle_{PbPb}}{\langle \pi^+ \rangle_{PbPb}}, \quad (1)$$

$$\eta_p \equiv \frac{R_p}{R_{Pb}}, \quad \eta_A \equiv \frac{R_A}{R_{Pb}}, \quad (2)$$

where  $\langle \dots \rangle_{pp}$  and  $\langle \dots \rangle_{AA}$ , or  $\langle \dots \rangle_{PbPb}$  correspond to the event averages in inelastic p+p and A+A or Pb+Pb collisions, respectively. Thereafter the symbol A+A refers to collisions of light and intermediate size nuclei. The data on  $R_p$  and  $R_{Pb}$  are presented in Fig. 1 as function of the center-of-mass energy of a nucleon pair  $\sqrt{s_{NN}}$ . In the left and right panels of Fig. 2 the energy dependence of  $\eta_p$  and  $\langle K^+ \rangle_{pp}$  are depicted. To calculate the  $\eta_p$  we use the  $R_{Pb}$  data presented

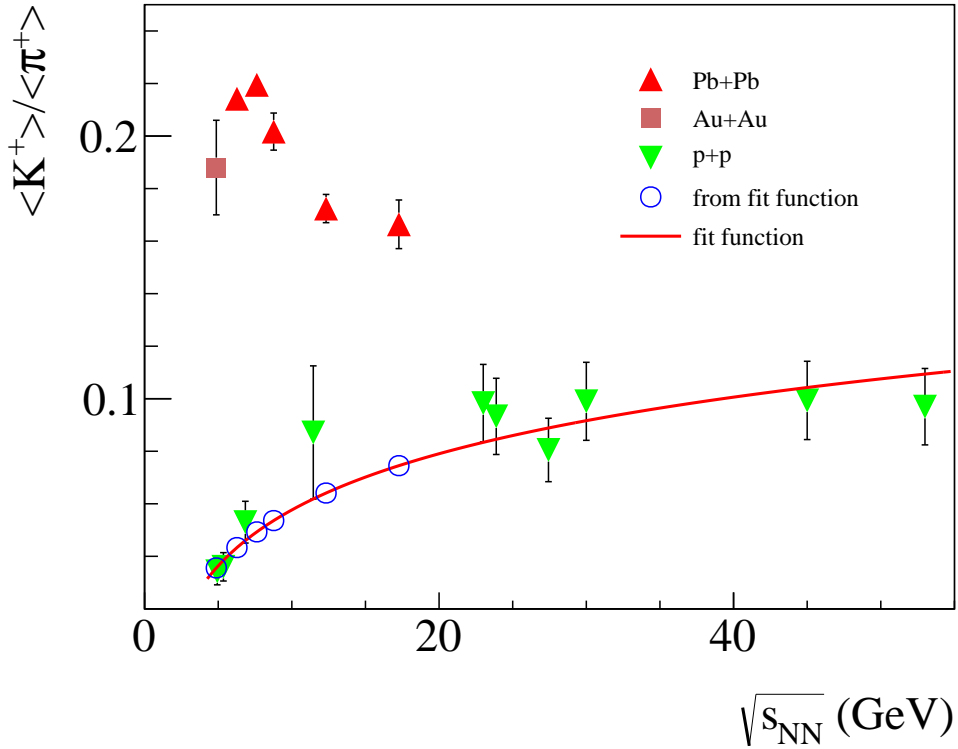


Figure 1. (Color Online) The  $K^+/\pi^+$  ratio in central Pb+Pb and Au+Au, and inelastic p+p collisions as a function of the center-of-mass energy  $\sqrt{s_{NN}}$  [7] .

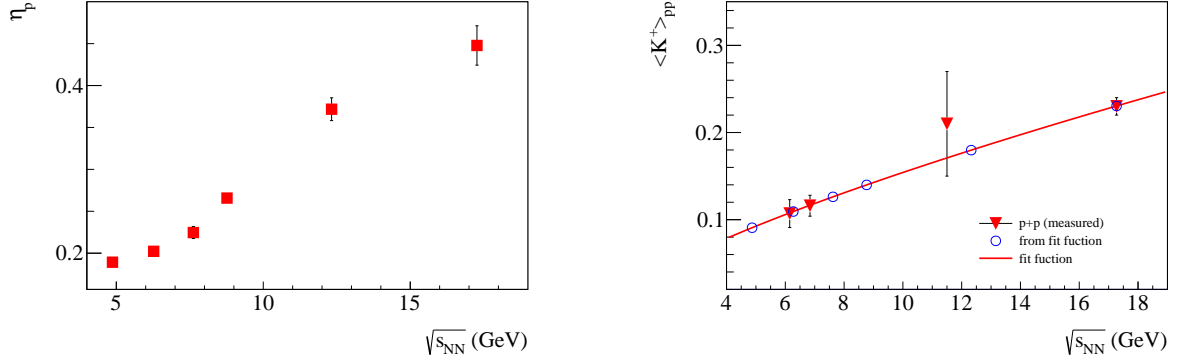


Figure 2. (Color Online) The strangeness suppression factor  $\eta_p$  (left panel) and the multiplicity  $\langle K^+ \rangle_{pp}$  [12] (right panel) as functions of  $\sqrt{s_{NN}}$ .

in Fig. 1 and a function  $a + b \cdot (\sqrt{s_{NN}})^c$  fitted to the p+p data and shown by the solid line. The parameters of the function are:  $a = -3.397$ ,  $b = 3.384$  and  $c = 0.009$ .

The net strangeness conservation requires equal number of strange quarks and antiquarks,  $N_s - N_{\bar{s}} = 0$ , in each event. The statistical model calculations take into account global conservation of the net strangeness. In the CE formulation a zero value of the net strangeness is fixed in each microscopic state of the statistical system. In GCE the chemical potential regulates only the average value of the net strangeness, i.e. the net strangeness is not necessarily vanishing in each microscopic state. Both statistical ensembles become equivalent in the thermodynamical limit when the system volume goes to infinity. This is discussed in detail in Appendix A.

The  $\pi^+$  multiplicity and the quantity  $z$  (see Appendix A, Eq. (15)) can be presented as:

$$\langle \pi^+ \rangle_{ii} = V_i n_{\pi^+}, \quad z_i = V_i n_s, \quad (3)$$

where  $i=p, A$ , or  $Pb$ . The  $\langle \pi^+ \rangle_{ii}$  and  $z_i$  correspond, respectively, to the GCE  $\pi^+$  multiplicity and  $\langle N_s \rangle_{gce} = \langle N_{\bar{s}} \rangle_{gce}$  in  $i + i$  collisions. Note that strange (anti)quark multiplicity  $\langle N_s \rangle_{gce}$  corresponds to the complete strangeness equilibration and does not yet take into account the CE suppression effects. We assume that the values of the pion number density  $n_{\pi^+} = \langle \pi^+ \rangle / V$  and the strange (anti)quark number density  $n_s = \langle N_s \rangle_{gce} / V$  are not sensitive to the type of reactions, i.e. they have the same values in p+p, A+A, and Pb+Pb collisions at the same collision energy. The volumes  $V_i$  are, however, different in each of these  $i + i$  reactions, and they are assumed to be proportional to the number of wounded nucleons  $N_W$  ( $N_W = 2$  in inelastic

p+p collisions). The GCE formulation will be adopted for pion multiplicity in all types of  $i + i$  collisions. The total number of negatively charged particles is larger than one (even in p+p collisions) at the SPS energies. Therefore, the CE effects of electric charge conservation are small and can be neglected. To calculate  $\langle N_s \rangle = \langle N_{\bar{s}} \rangle$  both the CE effects and the incomplete strangeness equilibration are considered. This is discussed in Appendix A (see Eq. (18)). For the  $K^+$  multiplicity it then follows:

$$\langle K^+ \rangle_{ii} = \frac{1}{2} \gamma_S^i z_i \frac{I_1(2\gamma_S^i z_i)}{I_0(2\gamma_S^i z_i)}, \quad (4)$$

where the relation  $\langle K^+ \rangle \cong 0.5N_{\bar{s}}$  has been used.

Finally, we obtain the following expressions for  $\langle K^+ \rangle_{pp}$  and  $\eta_p$  in p+p collisions:

$$\langle K^+ \rangle_{pp} = \frac{1}{2} \gamma_S^p z_p \frac{I_1(2\gamma_S^p z_p)}{I_0(2\gamma_S^p z_p)}, \quad (5)$$

$$\eta_p = \frac{\gamma_S^p}{\gamma_S^{Pb}} \frac{I_1(2\gamma_S^p z_p)}{I_0(2\gamma_S^p z_p)}. \quad (6)$$

The above equations assume: (i) the same  $n_s$  and  $n_{\pi^+}$  GCE values of the particle number densities, as defined in Eq. (3) in p+p, A+A, and Pb+Pb collisions; (ii) the incomplete strangeness equilibration regulated by  $\gamma_S^i$  in  $i + i$  collisions ( $i = p, A$ , and Pb); (iii) the relation  $I_1/I_0 \cong 1$  is adopted in central Pb+Pb collisions, as  $\gamma_S^{Pb} z_{Pb} \gg 1$ .

### III. PREDICTIONS FOR LIGHT ION COLLISIONS

The left-hand-sides of Eqs. (5) and (6) involve quantities which have been experimentally measured. The energy dependences of  $\langle K^+ \rangle_{pp}$  and  $\eta_p$  are shown in Fig. 2. For the  $\langle K^+ \rangle_{pp}$  we used the fit function  $a \cdot (\sqrt{s_{NN}})^b$  with  $a=0.028$  and  $b=0.736$  presented by the solid line in the right panel of Fig. 2. All in all there are 3 unknowns,  $\gamma_S^p$ ,  $z_p$ , and  $\gamma_S^{Pb}$ , entering to the right-hand-sides of Eqs. (5) and (6). However, they can be combined as

$$X = \gamma_S^p z_p, \quad Y = \gamma_S^p / \gamma_S^{Pb}. \quad (7)$$

Together with Eq. (7), Eqs. (5) and (6) represent the system of two equations with two unknown quantities:

$$\langle K^+ \rangle_{pp} = \frac{1}{2} X \frac{I_1(2X)}{I_0(2X)}, \quad (8)$$

$$\eta_p = Y \frac{I_1(2X)}{I_0(2X)}. \quad (9)$$

The solution of the transcendental Eq. (8),  $X = X(\sqrt{s_{NN}})$ , is shown in the left panel of Fig. 3. On the other hand, Eq. (9) gives the value of  $Y = \eta_p I_0(2X)/I_1(2X)$  presented in the right panel of Fig. 3.

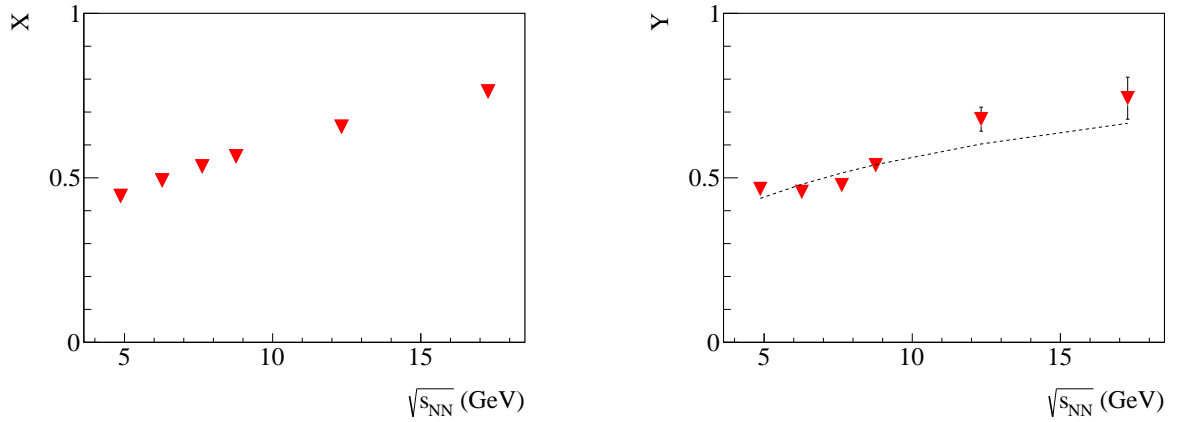


Figure 3. (Color Online) The energy dependence of the solutions  $X$  and  $Y$  of Eqs. (8), (9). Left panel:  $X = \gamma_S^p z_p$ . Right panel:  $Y = \gamma_S^p / \gamma_S^{Pb}$ . The dashed line represents the fit with the Eq. (11), yielding  $\alpha = 1.015$  and  $\beta = 0.189$ .

Assuming now  $z_A = z_p \cdot N_W/2$ , where  $N_W$  is the average number of wounded nucleons in A+A collisions, one can calculate the  $K^+$  to  $\pi^+$  ratio as:

$$R_A \equiv \frac{\langle K^+ \rangle_{AA}}{\langle \pi^+ \rangle_{AA}} = R_{Pb} \times \frac{\gamma_S^A}{\gamma_S^{Pb}} \cdot \frac{I_1(2\gamma_S^A z_p \cdot N_W/2)}{I_0(2\gamma_S^A z_p \cdot N_W/2)} = R_{Pb} \times \frac{\gamma_S^A}{\gamma_S^{Pb}} \cdot \frac{I_1[(\gamma_S^A/\gamma_S^p) X \cdot N_W]}{I_0[(\gamma_S^A/\gamma_S^p) X \cdot N_W]}. \quad (10)$$

Next, following the prescription of Ref. [13], we used the following expression for the dependence of  $\gamma_S^A$  on  $N_W$  and  $\sqrt{s_{NN}}$ :

$$\gamma_S^A = 1 - \alpha \exp \left[ -\beta \sqrt{N_W \sqrt{s_{NN}}} \right] \quad (11)$$

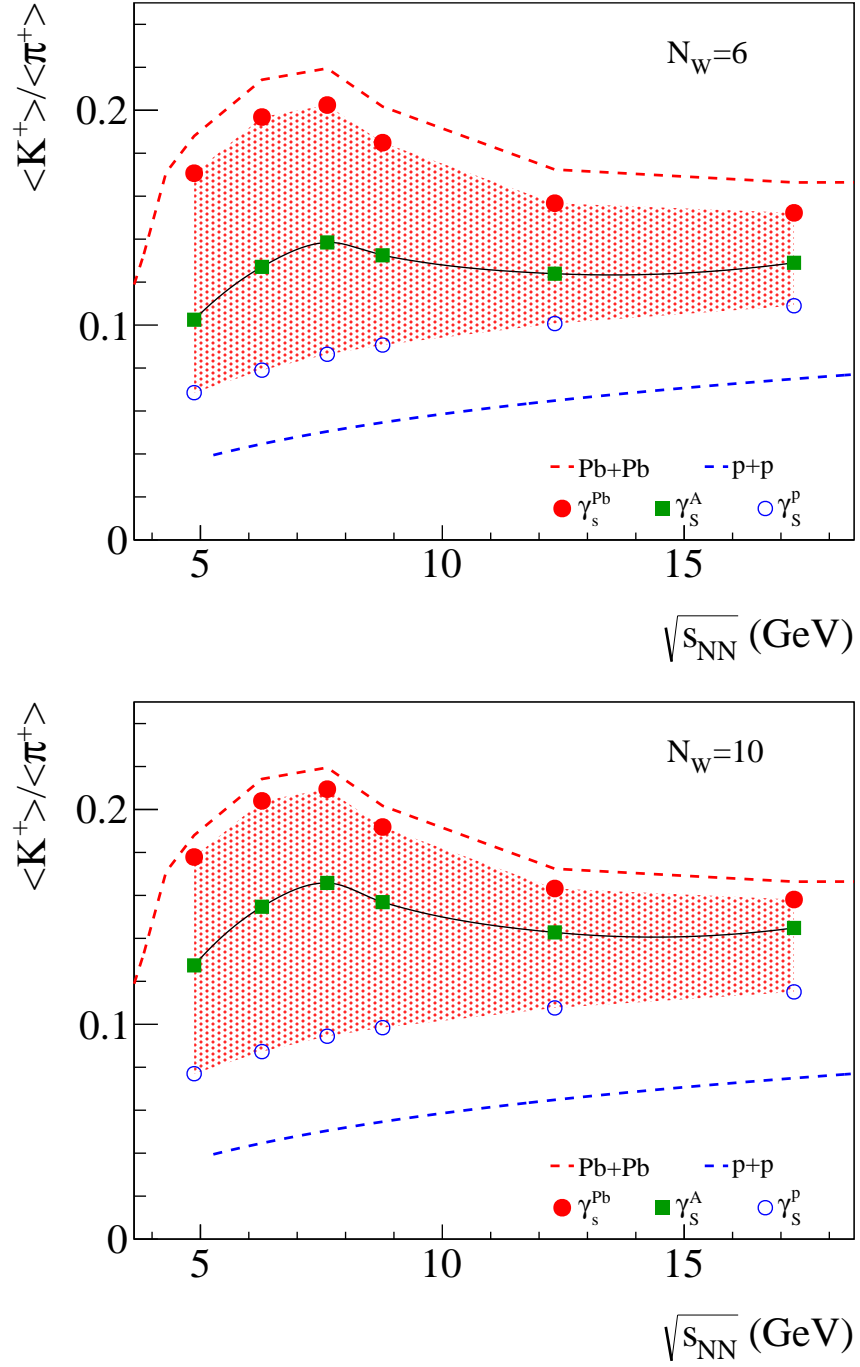


Figure 4. (Color online) The energy dependence of  $R_A$  as calculated by Eq.(10) for  $N_W = 6$  (upper panel) and  $N_W = 10$  (lower panel) are presented with green boxes. The dashed lines represent measurements in p+p (lower line) and Pb+Pb (upper line) collisions. The lower (open circles) and upper (full circles) limits are calculated using Eqs. (12) and (13), respectively.



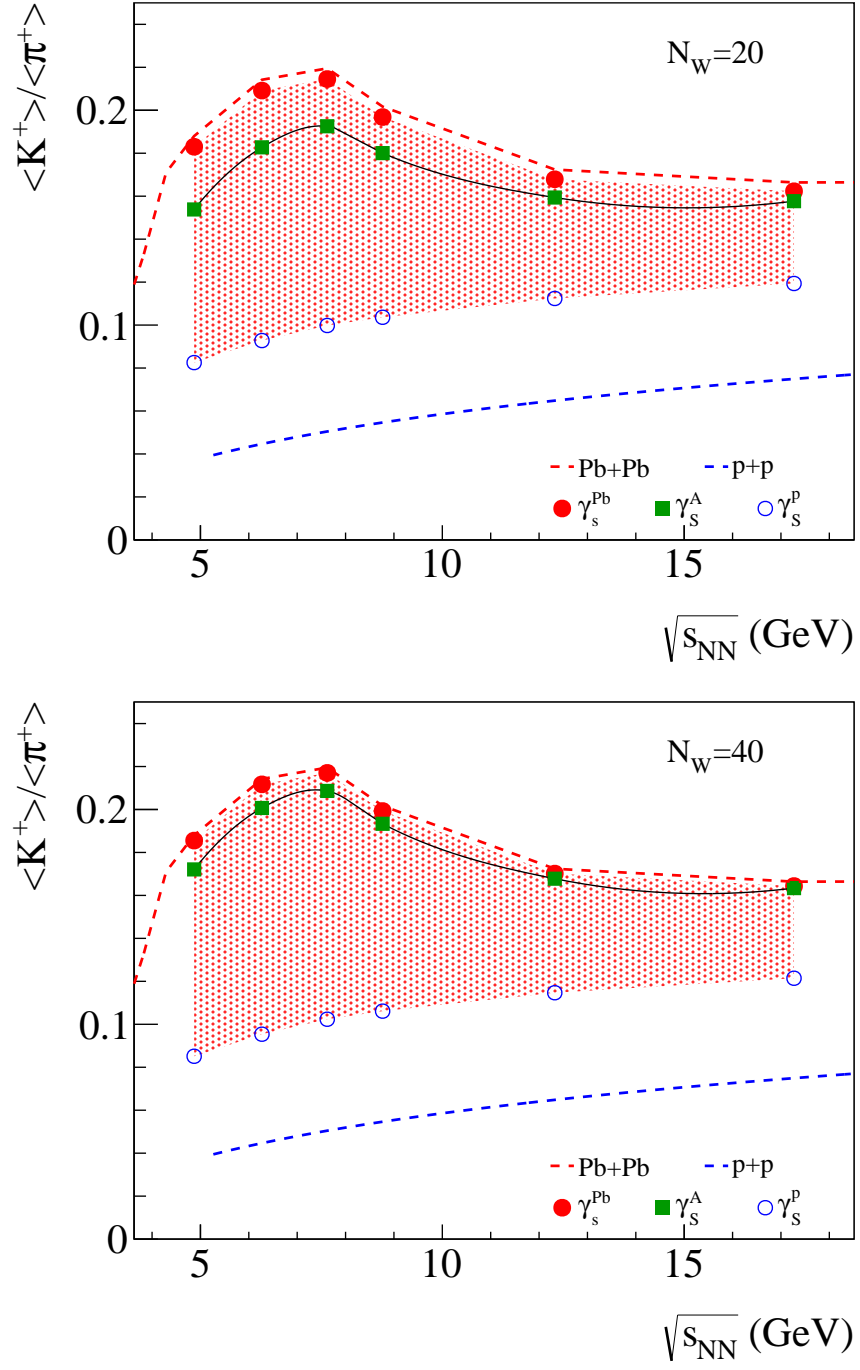


Figure 5. (Color Online) The same as in Fig. 4 but for  $N_W = 20$  (upper panel) and  $N_W = 40$  (lower panel).

with  $\alpha=1.015$  and  $\beta = 0.189$ , which were obtained by fitting the  $\gamma_s^p/\gamma_s^{Pb}$  ratio (see the right

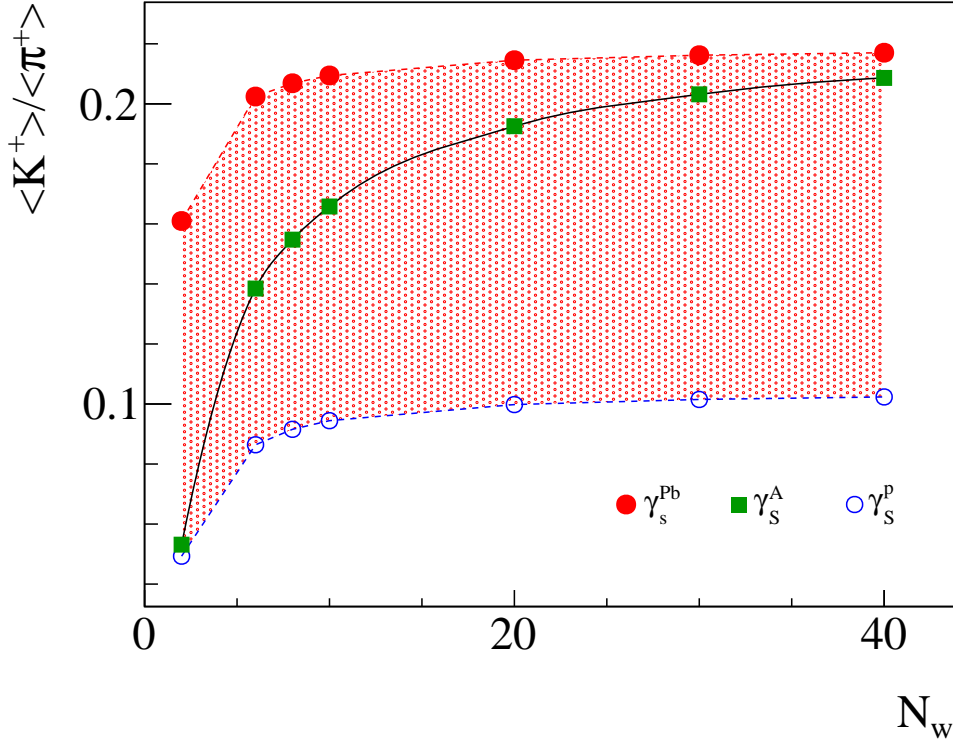


Figure 6. (Color Online) The dependence of  $\langle K^+ \rangle / \langle \pi^+ \rangle$  on the number of wounded nucleons  $N_W$  in A+A collisions at fixed energy of  $\sqrt{s_{NN}} = 7.6$  GeV are presented with green boxes. The lower (open circles) and upper (full circles) limits are calculated using Eqs. (12) and (13), respectively.

panel of Fig. 3).

Furthermore, taking  $\gamma_S^A = \gamma_S^p$  and  $\gamma_S^A = \gamma_S^{Pb}$ , we obtain the lower ( $R_A^{\text{low}}$ ) and upper ( $R_A^{\text{up}}$ ) limits for  $R_A$  defined in Eq. (10):

$$R_A^{\text{low}} = R_{Pb} \times Y \cdot \frac{I_1[X \cdot N_W]}{I_0[X \cdot N_W]}, \quad (12)$$

$$R_A^{\text{up}} = R_{Pb} \times \frac{I_1[Y^{-1} X \cdot N_W]}{I_0[Y^{-1} X \cdot N_W]}. \quad (13)$$

In Fig. 4 and Fig. 5 the energy dependence of  $R_A$  for A+A collisions with different numbers of wounded nucleons  $N_W$  are presented. The green boxes are calculated using Eqs. (10) and (11). The lower and upper dashed lines correspond to the  $K^+/\pi^+$  ratios in p+p and Pb+Pb collisions, respectively. The open and full circles are calculated using Eqs. (12) and (13), correspondingly.

In Fig. 6 we illustrate with green boxes the system size dependence (expressed in terms of wounded nucleons) of the  $\langle K^+ \rangle / \langle \pi^+ \rangle$  ratio at fixed energy of  $\sqrt{s_{NN}} = 7.6$  GeV. The upper limit (full circles) corresponds to  $\gamma_S^A = \gamma_S^{Pb}$  and the lower limit (open circles) to  $\gamma_S^A = \gamma_S^p$ . Interestingly, the  $\langle K^+ \rangle / \langle \pi^+ \rangle$  ratio becomes approximately independent of the number of wounded nucleons for  $N_W > 40$ .

#### IV. SUMMARY

In summary, the  $K^+/\pi^+$  ratio in p+p and Pb+Pb collisions is considered within the statistical model. The model takes into account the net strangeness conservation within the canonical ensemble formulation and the incomplete total strangeness equilibration regulated by the parameter  $\gamma_S$ . Both effects are assumed to depend on the system size only. The two model parameters are extracted from the existing data in p+p and Pb+Pb collisions. We present the model estimates for the lower and upper limits of  $R_A$ , defined in Eq. (10), for A+A collisions which correspond to  $\gamma_S^A = \gamma_S^p$  and  $\gamma_S^A = \gamma_S^{Pb}$ , respectively. Assuming a functional dependence of  $\gamma_S^A$  on  $N_W$  and  $\sqrt{s_{NN}}$  in the form of Eq. (11) we managed to make definite predictions for the  $K^+/\pi^+$  ratio in collisions of light and intermediate nuclei at the SPS energy region. We hope that our estimates will be helpful for the NA61 SHINE program with collisions between light and intermediate size nuclei. In particular, the deviations of the future experimental results from our predictions, if there will be any, will clearly underline important physics differences between p+p and A+A collisions.

#### ACKNOWLEDGMENTS

We would like to thank Marek Gaździcki, Francesco Becattini and Herbert Ströbele for fruitful discussions and comments. The work of M.I.G. was supported by the Program of Fundamental Research of the Department of Physics and Astronomy of NAS, Ukraine, and by the State Agency of Fundamental Research of Ukraine, Grant F58/04. A.R. gratefully acknowledges the support by the German Research Foundation (DFG Grant No. GA 1480/2.1).

## APPENDIX

The GCE partition function for strange quarks and antiquarks reads

$$\begin{aligned} Z_{gce}(T, V, \gamma_S; \lambda, \bar{\lambda}) &= \sum_{N_s=0}^{\infty} \sum_{N_{\bar{s}}=0}^{\infty} \frac{(\gamma_S \lambda z)^{N_s}}{N_s!} \frac{(\gamma_S \bar{\lambda} z)^{N_{\bar{s}}}}{N_{\bar{s}}!} \\ &= \exp\left(\gamma_S \lambda z + \gamma_S \bar{\lambda} z\right) \rightarrow \exp\left(2\gamma_S z\right), \end{aligned} \quad (14)$$

where the quantity  $z$  is the so-called one-particle partition function

$$z = \frac{V}{\pi^2} T m_s^2 K_2\left(\frac{m_s}{T}\right) \equiv V \cdot n_s. \quad (15)$$

In Eqs. (14), (15),  $V$  and  $T$  are the system volume and temperature, respectively,  $m_s$  is the mass of strange (anti)quark and  $K_2$  is the modified Bessel function. Furthermore, the Boltzmann approximation is used because the quantum statistics effects are negligible. The  $\lambda$  and  $\bar{\lambda}$  in Eq. (14) are auxiliary parameters introduced to calculate  $N_s$  and  $N_{\bar{s}}$  averages:

$$\langle N_s \rangle_{gce} = \left[ \frac{\partial \ln Z_{gce}}{\partial \lambda} \right]_{\lambda=\bar{\lambda}=1} = \langle N_{\bar{s}} \rangle_{gce} = \left[ \frac{\partial \ln Z_{gce}}{\partial \bar{\lambda}} \right]_{\lambda=\bar{\lambda}=1} = \gamma_S z, \quad (16)$$

The parameter  $\gamma_S$  regulates the strangeness equilibration [9]. It is used to fit the average value of the total strangeness measured by experiments:  $\gamma_S < 1$  corresponds to an incomplete strangeness equilibration, whereas  $\gamma_S = 1$  means a complete chemical equilibrium.

The GCE partition function (see Eq. (14)) leads to the equal average values of  $N_s$  and  $N_{\bar{s}}$ . However, the terms with  $N_s \neq N_{\bar{s}}$  contribute to  $Z_{gce}$ . On the other hand, the CE partition function requires  $N_s = N_{\bar{s}}$  in each microscopic state of the system:

$$\begin{aligned} Z_{ce}(T, V, \gamma_S; \lambda, \bar{\lambda}) &= \sum_{N_s=0}^{\infty} \sum_{N_{\bar{s}}=0}^{\infty} \frac{(\gamma_S \lambda z)^{N_s}}{N_s!} \frac{(\gamma_S \bar{\lambda} z)^{N_{\bar{s}}}}{N_{\bar{s}}!} \delta(N_s - N_{\bar{s}}) \\ &= \frac{1}{2\pi} \int_0^{2\pi} d\phi \exp\left[\gamma_S z (\lambda e^{i\phi} + \bar{\lambda} e^{-i\phi})\right] \rightarrow I_0(2\gamma_S z). \end{aligned} \quad (17)$$

The average numbers of strange quarks and antiquarks become:

$$\langle N_s \rangle_{ce} = \left[ \frac{\partial \ln Z_{ce}}{\partial \lambda} \right]_{\lambda=\bar{\lambda}=1} = \langle N_{\bar{s}} \rangle_{ce} = \left[ \frac{\partial \ln Z_{ce}}{\partial \bar{\lambda}} \right]_{\lambda=\bar{\lambda}=1} = \gamma_S z \cdot \frac{I_1(2\gamma_S z)}{I_0(2\gamma_S z)}. \quad (18)$$

The ratio of Bessel functions  $I_1$  and  $I_0$  in Eq. (18) describes the suppression effect due to conservation of the net strangeness in each microscopic state of the CE. The CE suppression

factor  $I_1/I_0$  is a function of  $\gamma_S z$ . Thus, only this quantity defines the CE effects, the specific values of  $m_s$ ,  $T$ , and  $V$  are irrelevant. For  $\gamma_S z \gg 1$  it follows that  $I_1(2\gamma_S z)/I_0(2\gamma_S z) \cong 1$ . Therefore, for large systems, the CE suppression effects are negligible, i.e., the CE and GCE multiplicities become identical.

- 
- [1] A. Bialas, M. Bleszynski, W. Czyz, Nucl. Phys. B **111**, 461 (1976).
  - [2] B. Müller and J. Rafelski, Phys. Rev. Lett. **48**, 1066 (1982); P. Koch, B. Müller, and J. Rafelski, Phys. Rep. **142**, 321 (1986).
  - [3] M. Gaździcki and M.I. Gorenstein, Acta Phys. Pol. B **30**, 2705 (1999).
  - [4] C. Alt *et al.* [NA49 Collaboration], Phys. Rev. C **77**, 024903 (2008) (and references therein).
  - [5] M. Gaździcki, M.I. Gorenstein, and P. Seyboth, Acta Phys. Pol. B **42**, 307 (2011).
  - [6] A. Rustamov, Central Eur. J. Phys. **10**, 1267-1270 (2012), arXiv:1201.4520v1 [nucl-ex] (2012)
  - [7] C. Alt et al. (NA49 Collaboration), Phys. Rev. C **77**, 024903 (2008)
  - [8] J. Rafelski and M. Danos, Phys. Lett. B **97**, 279 (1980); J. Clymans, K. Redlich, and E. Suhonen, Z. Phys. C **51**, 137 (1991); F. Becattini, Z. Phys. C **69**, 485 (1996) and Nucl. Phys. Proc. Suppl. **92**, 137 (2001); F. Becattini and U. Heinz, Z. Phys. C **76**, 269 (1997); M.I. Gorenstein, M. Gaździcki, and W. Greiner, Phys. Lett. B **483**, 60 (2000); M.I. Gorenstein, A.P. Kostyuk, H. Stöcker, and W. Greiner, Phys. Lett. B **509**, 277 (2001).
  - [9] J. Rafelsky, Phys. Lett. B **62**, 333 (1991).
  - [10] F. Becattini, P. Castorina, A. Milov, and H. Satz, Eur. Phys. J. C **66**, 377 (2010); F. Becattini, Physics of Atomic Nuclei, **75**, No. 5, 646 (2012).
  - [11] NA61 Collaboration, CERN-SPSC-2012 (2012)
  - [12] M. Gaździcki and D. Röhrich, Z. Phys. C **71**, 55 (1996)
  - [13] F. Becattini, J. Mannien, and M. Gaździcki, Phys. Rev. C **73**, 044905 (2006).